PAPER • OPEN ACCESS

The stability of hole-doped antiferromagnetic state in a two-orbital model

New Journal of Physics
The open access journal at the forefront of physics

Deutsche Physikalische Gesellschaft DPG
IOP Institute of Physics

Published in partnership with: Deutsche Physikalische Gesellschaft and the Institute of Physics

OPEN ACCESS

RECEIVED
15 January 2020

REVISED
23 March 2020

ACCEPTED FOR PUBLICATION
30 March 2020

PUBLISHED
24 June 2020

PAPER

The stability of hole-doped antiferromagnetic state in a two-orbital model

Dheeraj Kumar Singh[1,2,3,6], **Ara Go**[4], **Han-Yong Choi**[5] **and Yunkyu Bang**[2,3,6]

[1] School of Physics and Materials Science, Thapar Institute of Engineering and Technology, Patiala-147004, Punjab, India
[2] Department of Physics, POSTECH, Pohang 790-784, Republic of Korea
[3] Asia Pacific Center for Theoretical Physics, Pohang, Gyeongbuk 790-784, Republic of Korea
[4] Center for Theoretical Physics of Complex Systems, Institute for Basic Science (IBS), Daejeon 34051, Republic of Korea
[5] Department of Physics and Institute for Basic Science Research, SungKyunKwan University, Suwon 440-746, Republic of Korea
[6] Authors to whom any correspondence should be addressed.

E-mail: dheeraj.kumar@thapar.edu and ykbang@apctp.org

Keywords: cuprates, Hund's coupling, spin-wave excitations, antiferromagnetic state

Abstract

We investigate the hole-doped antiferromagnetic state in a two-orbital model of cuprates. The model also includes $d_{3z^2-r^2}$ orbital. Unlike the one-orbital model, we find the antiferromagnetic state stable against the hole doping for the cuprates with orbital splitting between $d_{x^2-y^2}$ and $d_{3z^2-r^2}$ orbitals being $\sim$1 eV. This results from the fact that the Hund's coupling enforces the filling of $d_{x^2-y^2}$ orbital $\approx$1 indicated by a significant reduction of $d_{x^2-y^2}$ spectral density at the Fermi level. This, in turn, leads to the suppression of intraband fluctuations detrimental to the antiferromagnetic phase. In this scenario, hole doping involves removal of mainly $d_{3z^2-r^2}$ electrons that are comparatively more localized. One important caveat of our meanfield theoretic result and conclusion is that they are reliable only for a very low hole doping region.

After more than thirty years of discovery of cuprates exhibiting high-T_c superconductivity [1], several aspects of their behavior could not be understood within the one-orbital Hubbard model. This is despite the considerable success of the latter in being able to capture the low-energy physics [2]. Various spectroscopic methods indicate that the doped holes may be located on the oxygen sites through the so called *charge-transfer* mechanism. The mechanism basically involves the positioning of oxygen (O) p band above the lower Hubbard band. Therefore, a more realistic description requires the three-orbital model which also incorporates O–p orbitals in the CuO_2 sheet. Further, it was argued that the physics of the d–p model could effectively be understood within one-orbital model. That is, the doped hole was shown to be localized within the square formed by O atoms and Cu^+ at the center. In other words, d–p hybridization leads to the formation of so called *Zhang-Rice singlet* [3, 4]. Physics of cuprates has also been studied within the three-orbital models where it's limitation in explaining the high-energy optical absorption spectrum was noted [5].

One of the prominent limitations of the one-orbital model was it's inability to describe the hole-doped antiferromagnet (AFM) [6]. Such a state obtained within the standard meanfield theories is not stable against the transverse-spin fluctuations or spin twisting. Other possibilities such as the stabilization of a spiral state with an ordering wavevector different from the magnetic ordering wavevector (π, π) was also ruled out [7, 8, 9, 10, 11, 12, 13]. Experimentally, a significant asymmetry exists in the doping vs temperature phase diagram of cuprates. But the AFM state does get stabilized in a sizable hole-doped region ($0 \lesssim x_h \lesssim 0.04$) even though the region is relatively smaller than that in the electron-doped region [14].

In this paper, we uncover several features associated with the two-orbital model based on $3d_{x^2-y^2}$ and $3d_{3z^2-r^2}$ orbitals with orbital splitting $\sim$1 eV such as in $La_{2-x}Sr_xCuO_4$. These features may be of significant importance in understanding the Mott and pseudogap physics of cuprates and similar systems. Our main findings are: (i) the hole-doped AFM state is robust against the spin twisting in the presence of a finite

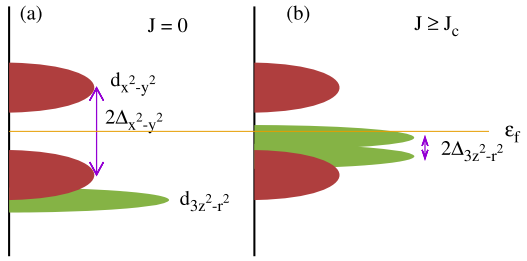

Figure 1. Schematic of magnetic exchange gap 2Δ in the hole-doped antiferromagnetic state of a two-orbital model. Two scenarios with Hund's coupling (a) $J = 0$ and (b) $J \gtrsim J_c$. Beyond a critical J_c, $d_{3z^2-r^2}$ shifts upward to the Fermi level while the contribution from $d_{x^2-y^2}$ is suppressed as the latter shifts downwards.

number of holes, a characteristics otherwise absent in the one orbital. We confirmed that by checking the stability of the AFM state by subjecting it to the transverse-spin fluctuations.

(ii) Electrons are removed from $d_{3z^2-r^2}$ orbital on doping holes, i.e, this orbital act as a charge reservoir. The behavior is similar to the charge-transfer mechanism involving O p orbital. The low-lying $d_{3z^2-r^2}$-band is shifted up above the lower $d_{x^2-y^2}$ band (figure 1). Two important consequences are: (a) electronic states appear near $(\pi, 0)$ instead of around $(\pi/2, \pi/2)$ [15, 16] and (b) the chemical potential is almost pinned because of the large spectral weight associated with narrow $d_{3z^2-r^2}$ band [14].

(iii) Both are direct consequences of the Hund's coupling or more specifically Hund's first rule which supports a maximum spin-configuration. Accordingly, the electrons should be removed from $d_{3z^2-r^2}$ orbital on doping and the charge density of $d_{x^2-y^2}$ orbital remains fixed at $\approx$1. As a result, a significant suppression of intraband spin fluctuations occurs, which is detrimental to the AFM state. Thus, various rich aspects of Hund's physics in the hole-doped cuprates with smaller orbital splitting are highlighted.

The necessity to include $d_{3z^2-r^2}$ orbital lying $\sim$1 eV below the Fermi level was invoked recently to explain the difference between the superconducting transition temperature (T_c) of $La_{2-x}(Sr,Ba)_xCuO_4$ and $HgBa_2CuO_{4+\delta}$ [17, 18]. The e_g orbitals splitting in the former is $\approx$1 eV while it is $\approx$2 eV in the latter. The splitting size is dependent on the distance of apical oxygen from CuO_2 plane [19]. For cuprates, the splitting between the two sets e_g and t_{2g} of orbitals is also $\approx$2 eV. Therefore, $d_{x^2-y^2}$ orbital based one-orbital model can describe the correlation effects for cuprates with larger e_g splitting, whereas it is important to include both e_g orbitals for those with smaller splitting.

Necessity of $d_{3z^2-r^2}$ orbital was also emphasized in order to describe certain features of magnon dispersion in the hole-doped La_2CuO_4, which otherwise could not be described within the one-orbital model [20]. A significant hybridization of bands involving $d_{3z^2-r^2}$ orbital has also been reported in the angle-resolved photoelectron spectroscopy (ARPES) experiments [21, 22].

All above observations indicate a multiorbital nature of the electrons in the cuprates. We, therefore, consider a two-orbital Hamiltonian including $d_{3z^2-r^2}$ orbital in addition to $d_{x^2-y^2}$ orbital:

$$\mathcal{H} = \sum_{\boldsymbol{ij}}\sum_{l,m}\sum_{\sigma} t_{\boldsymbol{ij}}^{lm} a_{\boldsymbol{i}l\sigma}^{\dagger} a_{\boldsymbol{j}m\sigma} + U\sum_{\boldsymbol{i},l} n_{\boldsymbol{i}l\uparrow} n_{\boldsymbol{i}l\downarrow} + \left(U' - \frac{J}{2}\right)\sum_{\boldsymbol{i},l<m} n_{\boldsymbol{i}l} n_{\boldsymbol{i}m} - 2J\sum_{\boldsymbol{i},l<m} \boldsymbol{S}_{\boldsymbol{i}l}\cdot\boldsymbol{S}_{\boldsymbol{i}m} + J\sum_{\boldsymbol{i},l<m,\sigma} a_{\boldsymbol{i}l\sigma}^{\dagger} a_{\boldsymbol{i}l\bar{\sigma}}^{\dagger} a_{\boldsymbol{i}m\bar{\sigma}} a_{\boldsymbol{i}m\sigma}. \tag{1}$$

$a_{\boldsymbol{i}l\sigma}^{\dagger}$ ($a_{\boldsymbol{i}l\sigma}$) is the creation (destruction) operators for electron with spin σ at site $\boldsymbol{i}$ in the orbital l, where $l \equiv d_{x^2-y^2}, d_{3z^2-r^2}$. The first term represents kinetic energy with $t_{\boldsymbol{ij}}^{lm}$ as hopping matrix elements from orbital l at site $\boldsymbol{i}$ to orbital m at site $\boldsymbol{j}$, respectively. They are listed in table 1 for La_{2-x} $(Sr/Ba)_xCuO_4$ (reference [17, 18]). We have introduced a slight modification so that all the parameters are reduced by a factor $f = 0.87$. This is primarily aimed to capture the correct high-energy scale of spin-wave excitations in accordance with the experiments. The second and third terms incorporate the intra- and inter-orbital Coulomb interaction, respectively. The fourth and fifth term represent the Hund's coupling and the pair hopping while the condition $U = U' + 2J$ is set in all the calculations below to ensure the rotational invariance in the orbital space.

The mean-field Hamiltonian in the (π, π) AFM state can be expressed as [23]

$$H_{\boldsymbol{k}} = \sum_{\boldsymbol{k}\sigma} \Phi_{\boldsymbol{k}\sigma}^{\dagger} \begin{bmatrix} \hat{h}_{\boldsymbol{k}} + \hat{N} & \mathrm{sgn}\,\bar{\sigma}\hat{\Delta} \\ \mathrm{sgn}\,\bar{\sigma}\hat{\Delta} & \hat{h}_{\boldsymbol{k}+\boldsymbol{Q}} + \hat{N} \end{bmatrix} \Phi_{\boldsymbol{k}\sigma}, \tag{2}$$

Table 1. Hopping parameters within two-orbital model of cuprates. $t1$, $t2$, and $t3$ are the parameters corresponding to nearest, next nearest, next-next nearest neighbors hoppings in the unit of eV. The on site splitting between the two orbitals is 0.80 eV.

Hoppings	$t1$	$t2$	$t3$
$t^{11}(d_{x^2-y^2} \longleftrightarrow d_{x^2-y^2})$	−0.410	0.0811	−0.0639
$t^{12}(d_{x^2-y^2} \longleftrightarrow d_{3z^2-r^2})$	0.155	0.0	0.0224
$t^{22}(d_{3z^2-r^2} \longleftrightarrow d_{3z^2-r^2})$	−0.103	0	0

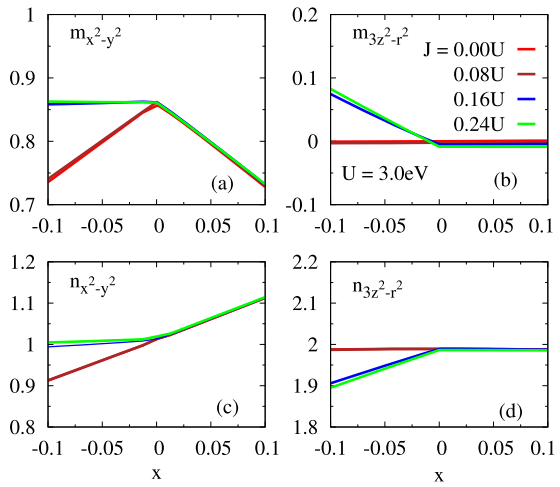

Figure 2. Orbital-resolved magnetization ((a) and (b)) and charge densities ((c) and (d)) as a function of electronic densities for different Hund's coupling J. Both m_ls and n_ls exhibit a linear dependence. The doping dependent behavior is remarkably different in the electron- and hole-doped regimes. At higher J, the magnetization and charge density in $d_{x^2-y^2}$ are almost constant, while the same change linearly for $d_{3z^2-r^2}$ orbital.

where $\Phi^\dagger_{\boldsymbol{k}\sigma} = (a^\dagger_{\boldsymbol{k}1\sigma}, a^\dagger_{\boldsymbol{k}2\sigma}, a^\dagger_{\boldsymbol{k}\bar{1}\sigma}, a^\dagger_{\boldsymbol{k}\bar{2}\sigma})$ with $a^\dagger_{\boldsymbol{k}\bar{l}\sigma} = a^\dagger_{\boldsymbol{k}+\boldsymbol{Q}l\sigma}$ and $\boldsymbol{Q} = (\pi, \pi)$. $\hat{h}_{\boldsymbol{k}}$ is the hopping matrix. The elements of the matrices $\hat{\Delta}$ and $\hat{N}$ are functions of the onsite interaction parameters, orbital magnetizations and charge densities. Elements of $\hat{\Delta}$ are $2\Delta_{ll} = Um_{ll} + J\sum_{l\neq m} m_{mm}$ and $2\Delta_{lm} = Jm_{lm} + (U-2J)m_{ml}$. Next, $2N_{ll} = Un_{ll} + (2U-5J)\sum_{l\neq m} n_{mm}$ and $2N_{lm} = Jn_{lm} + (4J-U)n_{ml}$. The charge densities and magnetizations are calculated as $n_{lm} = \sum_{\boldsymbol{k}\sigma}\langle a^\dagger_{\boldsymbol{k}l\sigma} a_{\boldsymbol{k}m\sigma}\rangle$ and $m_{lm} = \sum_{\boldsymbol{k}\sigma}\langle a^\dagger_{\boldsymbol{k}\bar{l}\sigma} a_{\boldsymbol{k}m\sigma}\rangle$ sgn σ. Summation over $\boldsymbol{k}$ is performed within the magnetic Brillouin zone. Eigenvalues and eigenvectors of the Hamiltonian matrix are used to calculate the order parameters in a self-consistent manner.

First, we examine the orbital charge densities and magnetization plotted as a function of carrier concentration in figure 2. For small J, the magnetization for $d_{x^2-y^2}$ first increases on moving from electron-doped region to hole-doped region. It reaches a maximum at zero doping and then decreases. On the other hand, the charge density decreases steadily all along. Meanwhile, there is no change in either of the quantities $m_{3z^2-r^2} \approx 0$ and $n_{3z^2-r^2} \approx 2.0$. This is not surprising because the corresponding band is placed well below the Fermi level ($E_b \approx -1.5$ eV) and the two orbitals are essentially decoupled in the absence of strong enough Hund's coupling. Therefore, the behavior of order parameters for $d_{x^2-y^2}$ orbital noted here is not different from what is expected in the one orbital case.

The features mentioned above can be noticed up to a critical $J_c \sim 0.1U$. Beyond that, however, a remarkable change occurs in the orbital-resolved magnetization and charge density for each of the orbitals. While the magnetization and the charge density remains unchanged in the electron-doped region, there is a role reversal in the hole-doped region. Inside the hole-doped region, neither the magnetization nor the charge density changes for $d_{x^2-y^2}$ orbital. In other words, the charge density and magnetization remain almost fixed at $n_{x^2-y^2} \approx 1.0$ and $m_{x^2-y^2} \approx 0.87$, respectively, even though the hole density increases. But the same does not hold for $d_{3z^2-r^2}$ as $m_{3z^2-r^2}$ increases while $n_{3z^2-r^2}$ decreases almost linearly. Note that a significant reduction in meanfield magnetization can occur due to the spin fluctuations [24–26]

To understand the unexpected behavior, we plot the density of states (DOS) in the hole-doped AFM state (see figures 3(a) and (b)). For smaller $J \lesssim J_c$, the Fermi level is located slightly below the top of lower $d_{x^2-y^2}$ band. At the same time, the DOS contribution due to $d_{3z^2-r^2}$ at the Fermi level is sharply peaked for $\approx$−1.5 eV. The scenario, however, changes dramatically for $J \gtrsim J_c$ (see figure 3(b)). The contribution at the

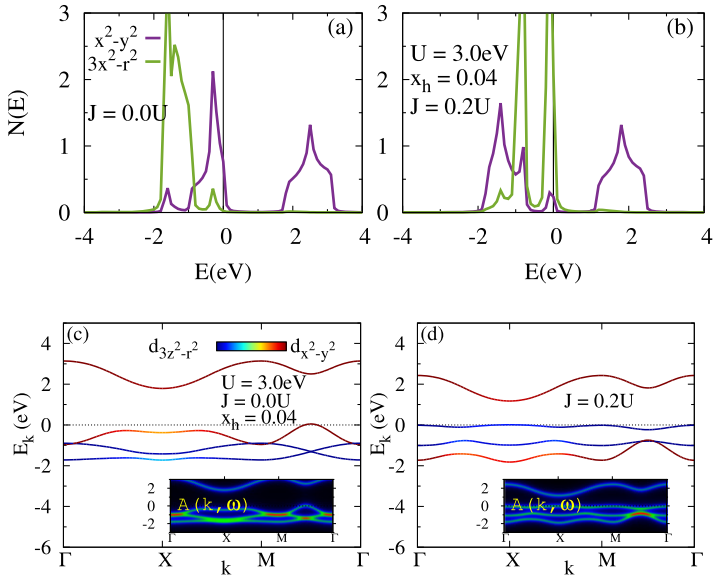

Figure 3. Orbital-resolved DOS for two cases (a) $J = 0$ and (b) $J = 0.2U$. The $d_{3z^2-r^2}$ DOS is sharply peaked near $\omega \approx -1.5$ eV with vanishing contribution at the Fermi level and electronic state appears around $(\pi/2, \pi/2)$. This is completely reversed for $J = 0.2U$, when $d_{x^2-y^2}$ DOS is suppressed and the electronic state of mainly $d_{3z^2-r^2}$ characteristics appear near $(\pi, 0)$. Exchange of position with respect to the Fermi level can be easily noticed for lower $d_{x^2-y^2}$ band and $d_{3z^2-r^2}$ band ((c) and (d)).

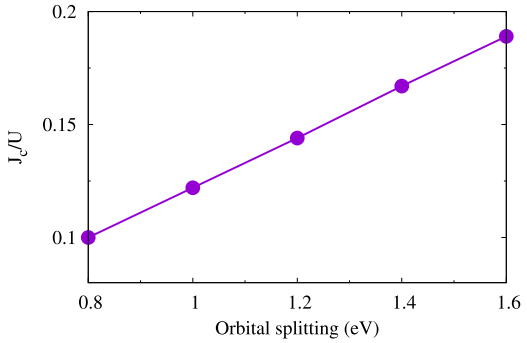

Figure 4. J_c shows a linear dependence on the orbital splitting between two orbitals $d_{x^2-y^2}$ and $d_{3z^2-r^2}$.

Fermi level due to $d_{x^2-y^2}$ orbital is now suppressed while that from $d_{3z^2-r^2}$ becomes dominant. This happens because the lower $d_{x^2-y^2}$ band and $d_{3z^2-r^2}$ band exchange their position (see figures 3(c) and (d)). Meanwhile, the asymmetry in the band structure is also suppressed. Both factors appears to be favorable for the AFM state. The exchange splitting for almost completely filled $d_{3z^2-r^2}$ band assumes a finite but non zero value because of a small magnetization.

The interorbital density-density interaction $\left(U' - J/2\right) n_{i1} n_{i2}$ is responsible for the exchange of position for lower $d_{x^2-y^2}$ band and $d_{3z^2-r^2}$ band. It can be easily seen by carrying out the meanfield decoupling of the term $\left(U' - J/2\right) n_{i1} n_{i2} \approx (U - 5J/2)(\langle n_2 \rangle n_1 + \langle n_1 \rangle n_2) + \text{const}$. The occupancies of the two orbital differ by ≈ 1, i.e, $\langle n_1 \rangle \approx 1$ and $\langle n_2 \rangle \approx 2$. This amounts to an orbital splitting of $\sim (-5J/2)(\langle n_2 \rangle - \langle n_1 \rangle) \approx -1.5$ eV (in comparison to when $J = 0$). This orbital splitting is exactly opposite to the one caused by ligand field, i.e., the apical oxygen height from CuO_2 plane.

The $d_{3z^2-r^2}$ DOS is sharply peaked because of relatively smaller intraorbital hopping in comparison to $d_{x^2-y^2}$. Moreover, the interorbital hopping is also very small and so is the hybridization. The extent of hybridization, which has remained a controversial issue, is hardly of any consequence for the results obtained here. We have checked it explicitly. However, the extent to which the $d_{3z^2-r^2}$ orbital is below the Fermi level in the unordered state is crucial for J_c as evident from figure 4 [27–37]. J_c can be seen to depend linearly on the orbital splitting.

The central implications of the above results are as follows. First of all, *orbital-selective* robustness of gap against hole doping for $d_{x^2-y^2}$ orbital is facilitated entirely by the Hund's exchange coupling between the two orbitals. This indicates the stability of doped-AFM state, which is possible for a realistic $J \sim 0.15U$.

There is a close resemblance with the orbital-selective Mottness. Latter can result from the fact that the hole resides on a significantly localized $d_{3z^2-r^2}$ orbital. Secondly, an additional scenario is made possible by the Hund's coupling for the charge-transfer like mechanism. Earlier proposals indicated that the doped holes may get transferred to oxygen atom. But when the e_g splitting is small, the holes may also display $d_{3z^2-r^2}$ orbital characteristics.

Our results also indicate that the nature of Mott transition unlike one orbital case is more complex mainly because of the additional player 'Hund's exchange interaction', which itself is a subject of intense current debate [38, 39]. The Hund's coupling is known to support a high-spin configuration. It also suppresses the double occupancy, a characteristics associated with the Mott transition near the half-filling in the one-orbital model. On the other hand, an increase in charge fluctuations may accompany with a reduction of quasiparticle spectral weight, a behavior contrary to what is observed in a one orbital model because of the strong correlation effects [40]. Thus, an important aspect of the Mott physics in the cuprates may also involve the suppression of orbital fluctuations or orbital decoupling as found to be important here [41, 42].

The stability of the hole-doped AFM state is already indicated by the fact that the $d_{x^2-y^2}$ orbital remains nearly half filled as well as $d_{x^2-y^2}$ orbital DOS is tiny at the Fermi level. In the following, however, we test the robustness of the meanfield state by subjecting it to the transverse spin fluctuations.

The transverse spin susceptibility for the two-orbital model is given by

$$\chi^{+-}_{\alpha\beta,lm}(\mathbf{q},\mathbf{q}',i\omega_n) = T\int_0^{1/T} d\tau e^{i\omega_n\tau}\langle T_\xi[\mathcal{S}^+_{\alpha\beta}(\mathbf{q},\tau)\mathcal{S}^-_{ml}(-\mathbf{q}',0)]\rangle. \tag{3}$$

$\mathbf{q},\mathbf{q}' = \mathbf{q}$ or $\mathbf{q}+\mathbf{Q}$ components of the spin operators in the Fourier space are given by $\mathcal{S}^i_{\alpha\beta}(\mathbf{q}) = \sum_{\mathbf{k}}\sum_{\sigma\sigma'} a^\dagger_{\alpha\sigma}(\mathbf{k}+\mathbf{q})\sigma^i_{\sigma\sigma'}a_{\beta\sigma'}(\mathbf{k})$. σ^i being Pauli matrices. Thus, the spin susceptibility for $\mathbf{q}' = \mathbf{q}$ is given in terms of Green's function as $\chi^{+-}_{\alpha\beta,lm}(\mathbf{q},\mathbf{q},i\omega_n) = \sum_{\mathbf{k},i\omega'_n} G^\uparrow_{\alpha l}(\mathbf{k}+\mathbf{q},i\omega'_n+i\omega_n)G^\downarrow_{m\beta}(\mathbf{k},i\omega'_n)$, where $G^\uparrow_{\alpha l}(\boldsymbol{k},i\omega_n)$ is obtained from the $\uparrow$-spin part of the meanfield Hamiltonian (equation (2)).

Within the random-phase approximation, the transverse-spin susceptibility in the (π,π)-AFM state is obtained as $\hat{\bar{\chi}}_{\rm RPA}(\mathbf{q},i\omega_n) = (\hat{\mathbf{1}} - \hat{\bar{\chi}}(\mathbf{q},i\omega_n)\hat{U})^{-1}\hat{\bar{\chi}}(\mathbf{q},i\omega_n)$, where $\hat{\mathbf{1}}$ is a 8×8 identity matrix. Interaction matrix is block diagonal and can be expressed as

$$\hat{U} = \begin{bmatrix} \hat{U}^o & \hat{O} \\ \hat{O} & \hat{U}^o \end{bmatrix}. \tag{4}$$

Elements of 4×4 matrix $\hat{U}^o$ are given as $U^o_{11;11} = U^o_{22;22} = U$, $U^o_{11;22} = U^o_{22;11} = U-2J$, $U^o_{12;12} = U^o_{21;21} = J$, and $U^o_{12;21} = U^o_{21;12} = J'$. $\hat{O}$ is a null matrix.

The bare-level susceptibility matrix in the AFM state is given by

$$\hat{\bar{\chi}}(\mathbf{q},i\omega_n) = \begin{bmatrix} \hat{\bar{\chi}}(\mathbf{q},\mathbf{q},i\omega_n) & \hat{\bar{\chi}}(\mathbf{q},\mathbf{q}+\mathbf{Q},i\omega_n) \\ \hat{\bar{\chi}}(\mathbf{q}+\mathbf{Q},\mathbf{q},i\omega_n) & \hat{\bar{\chi}}(\mathbf{q}+\mathbf{Q},\mathbf{q}+\mathbf{Q},i\omega_n) \end{bmatrix}, \tag{5}$$

where the elements in the ordered state are $\bar{\chi}_{\alpha\beta,lm} = \chi^{+-}_{\alpha\beta,lm} + \chi^{+-}_{\bar{\alpha}\beta,\bar{l}m} + \chi^{+-}_{\alpha\bar{\beta},l\bar{m}} + \chi^{+-}_{\bar{\alpha}\bar{\beta},\bar{l}\bar{m}}$. Note that the Umklapp processes are also included. Physical transverse-spin susceptibility can be calculated as $\bar{\chi}^{\rm ps}(\mathbf{q},i\omega_n) = \sum_{\alpha\mu}\bar{\chi}_{\alpha\alpha,\mu\mu}(\mathbf{q},\mathbf{q},i\omega_n)$ [43]. In the following, analytic continuation $i\omega_n \to \omega + i\eta$ with $\eta = 0.01$ eV is used throughout. Unit of energy is set to be eV.

Figure 5 shows $\mathrm{Im}\chi^{\rm ps}_{\rm RPA}(\mathbf{q},\omega)$ calculated in the two-orbital model as a function of Hund's coupling, where the hole doping is $x_{\rm h} = 0.04$ or total electron density is $n = 2.96$. As expected, the structure of spin-wave excitations for $J \lesssim J_{\rm c}$ (figure 5(a)) is same as one would expect for the one orbital model. Especially, there seem to exist zero energy modes besides the Goldstone mode with momenta shifted away from the ordering wavevector $\mathbf{Q}$. While the Goldstone mode for $\mathbf{Q}$ directly follows from the breaking of continuous spin-rotation symmetry, the existence of other nearby zero-energy modes $\mathbf{Q}'$ signals the presence of negative energy magnon branch. This implies the instability of the hole-doped AFM state. Presence of $d_{3z^2-r^2}$ orbital does not make any difference because of the reasons mentioned earlier.

The negative energy excitations branches signaling the instability of the hole-doped AFM state get suppressed beyond the critical $J \gtrsim J_{\rm c}$ (figure 5(b)). This should also be reflected in the spin-wave spectral weight distribution, where features with sharp peak may be noticed near and beyond $J_{\rm c}$. Thus, the stability of hole-doped AFM state is made possible by suppression of the intraband spin fluctuations in the lower $d_{x^2-y^2}$ band. Further, the intraband fluctuations coming mainly from the upper $d_{3z^2-r^2}$ band do not exhibit

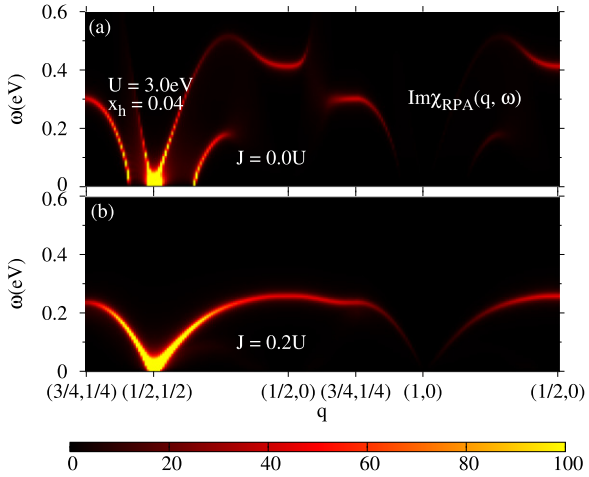

Figure 5. Behavior of spin-wave excitations as a function Hund's coupling (a) $J = 0.0U$ and (b) $J = 0.2U$ in the AFM state with hole concentration $x_h = 0.04$. Negative energy modes are absent of Hund's coupling $J \gtrsim J_c$ indicating the stability of the hole-doped AFM state.

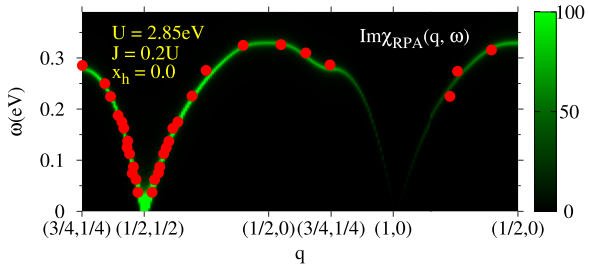

Figure 6. Comparison of calculated spin-wave dispersion within two-orbital model with the neutron-scattering data [44]. The intra-orbital Coulomb interaction parameter is taken to be 2.85 eV while the parameter $f = 0.96$ as defined in the text.

a hostility towards the AFM state. This bears a remarkable similarity to the electron-doped case in the one-orbital model with stabilized AFM state.

Although, we have demonstrated the stability of the hole-doped AFM state for $x_h \sim 0.04$, our conclusions remain valid for other fillings as well. For $x_h < 0.04$, the critical $J_c \sim 0.15U$ has a realistic value. However, the hole-doped region for stable AFM state may actually be small in view of other factors such as doping induced disorder and the ordering tendency towards d-wave superconductivity.

The role of Hund's coupling in stabilizing the magnetic phases such ferromagnet or stripe order is well known. In particular, J suppresses the quantum corrections. The suppression increases further with the number of orbitals, which leads to an enhanced stability of the ferromagnetic state [45, 46]. Moreover, role of J in stabilizing the striped magnetic order in iron pnictides against doping induced reduction in the Fermi surface nesting has also been pointed out [47–49]. Our results for the (π, π) type AFM state further highlight perhaps a general trend of stabilization of magnetic order by the Hund's coupling irrespective of the nature of spin arrangement in a multiorbital system. Therefore, it role should not be overlooked in multiorbital electron systems. In the present case, the stabilization of hole-doped AFM state is a direct result of the Hund's first rule which requires the maximization of total spin. This maximization can occur only when the electrons are removed from the completely filled $d_{3z^2-r^2}$ orbital instead of the half filled $d_{x^2-y^2}$ orbital.

Figure 6 shows the spin-wave dispersion obtained within the two-orbital model for $U = 2.85$ eV, $J = 0.2U$ and $f = 0.96$. For comparison, we have also shown the neutron scattering data [44]. For a realistic set of interaction and hopping parameters, we find a very good agreement with experimental data except the strong damping near (1/2, 0) as noted in a recent experiment [50]. Besides, the spin-wave excitation may have a non zero spin-wave spectral weight for $q_z \approx 0$ because of a very weak electronic dispersion along k_z [51].

We have also calculated the spin-wave dispersion for zero doping ($n = 3.00$) and electron-doped region ($n = 3.05$) as a function J (figure 7). For simplicity, we have set the intraorbital hopping for $d_{3z^2-r^2}$ zero. For electron doping, the AFM state is known to be stable in one-orbital model, a result which continues to hold

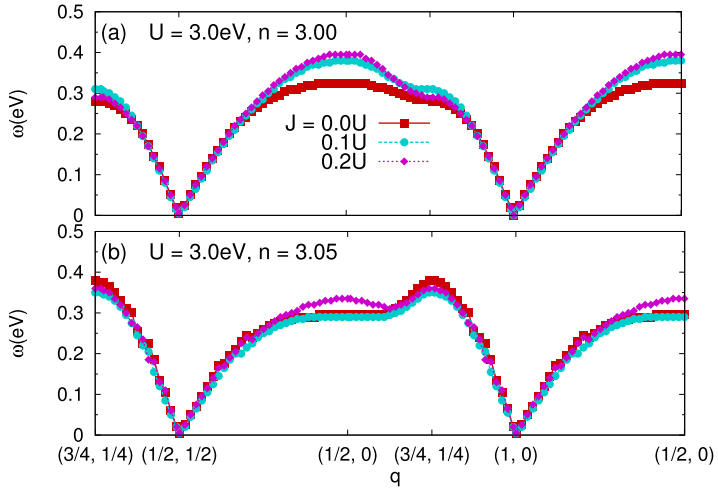

Figure 7. Spin-wave energies along different high-symmetry directions for various J when (a) $n = 3.00$ and (b) $n = 3.05$. For low-energy excitations, J dependence is almost absent. But a significant dependence can be noticed at higher energies particularly near $\mathbf{q} = (1/2, 0)$ and $(3/4, 1/4)$.

even in the two-orbital model. Thus, the spin-wave excitation is well defined for any J in the electron-doped regime as in the one-orbital case. It can be seen that J affects the high energy modes near high-symmetry points like (1/2, 0) or (3/4, 1/4) significantly with increase in their energy while low-energy excitations remains largely untouched. More or less a similar behavior is observed in the electron-doped region. The spin-wave excitations may show dependence on the orbital-splitting size as indicated in an RIXS (resonant inelastic x-ray scattering) study [20].

Although our work is based on the static meanfield approximation, it provides a new insight into the role of Hund's coupling in stabilizing the AFM state at low temperature. Further insight into the role of Hund's coupling on the nature of Mott transition can be obtained with the help of theoretical tools such as dynamical meanfield theory (DMFT) or meanfield theory based on the slave-spin approximation. The former one has been used but in the absence of Hund's coupling [52]. The slave-spin approximation also has been successful in describing the Mottness near integer fillings for various multiorbital systems [5]. It is to be noted that for higher doping our mean-field calculations become less reliable because of the charge fluctuations, which is largely suppressed in our approach, becomes more important.

In conclusions, we have investigated stability of the hole-doped AFM state in a two-orbital model for cuprates. The instability existent in the one-orbital model on hole doping is removed largely because of the Hund's coupling. Our results show that the doped holes may also occupy $d_{3z^2-r^2}$ orbital in addition to the oxygen p orbitals. This is possible because of shifting of low-lying $d_{3z^2-r^2}$ band up above the lower Hubbard split $d_{x^2-y^2}$ band. The feature appears similar to the charge-transfer mechanism with an important difference that the oxygen p band is unaffected or does not shift. Thus, our work highlights the crucial role of Hund's coupling in the cuprates with relatively smaller splitting of e_g orbitals $d_{x^2-y^2}$ and $d_{3z^2-r^2}$.

Acknowledgments

We acknowledge the use of HPC clusters at HRI. DKS would like to thank A Akbari for useful discussions. YB was supported through NRF Grant No. 2020-R1A2C2-007930 and No. 2019-R1H1A2-079920 funded by the National Research Foundation of Korea. AG is supported by the Institute for Basic Science under Grants No. IBS-R024-D1.

References

[1] Bednorz J G and Müller K A 1986 *Z. Phys.* B **64** 189
[2] Dagotto E 1994 *Rev. Mod. Phys.* **66** 763
[3] Zhang F C and Rice T M 1988 *Phys. Rev.* B **37** 3759
[4] Emery V J and Reiter G 1988 *Phys. Rev.* B **38** 4547
[5] de' Medici L, Wang X, Capone M and Millis A J 2009 *Phys. Rev.* B **80** 054501
[6] Lee P A, Nagaosa N and Wen X-G 2006 *Rev. Mod. Phys.* **78** 17
[7] Weng Z Y and Ting C S 1990 *Phys. Rev.* B **42** 803
[8] Krishnamurthy H R, Jayaprakash C, Sarker S and Wenzel W 1990 *Phys. Rev. Lett.* **64** 950
[9] Sarker S, Jayaprakash C, Krishnamurthy H R and Wenzel W 1991 *Phys. Rev.* B **43** 8775

[10] Singh A and Tešanović Z, Kim Ju H 1991 *Phys. Rev.* B **44** 7757
[11] Singh A and Tešsanović Z 1990 *Phys. Rev.* B **41** 614
[12] Auerbach A and Larson B E 1991 *Phys. Rev.* B **43** 7800
[13] Eberlein A, Metzner W, Sachdev S and Yamase H 2016 *Phys. Rev. Lett.* **117** 187001
[14] Damascelli A, Hussain Z and Shen Z-X 2003 *Rev. Mod. Phys.* **75** 473
[15] Ino A, Kim C, Nakamura M, Yoshida T, Mizokawa T, Shen Z-X, Fujimori A, Kakeshita T, Eisaki H and Uchida S 2000 *Phys. Rev.* B **62** 4137
[16] Zhou X J *et al* 2001 *Phys. Rev. Lett.* **86** 5578
[17] Sakakibara H, Usui H, Kuroki K, Arita R and Aoki H 2010 *Phys. Rev. Lett.* **105** 057003
[18] Sakakibara H, Usui H, Kuroki K, Arita R and Aoki H 2012 *Phys. Rev.* B **85** 064501
[19] Peng Y Y *et al* 2017 *Nat. Phys.* **13** 1201
[20] Ivashko O *et al* 2019 *Nat. Commun.* **10** 786
[21] Matt C E *et al* 2018 *Nat. Commun.* **9** 972
[22] Kramer K P *et al* 2019 *Phys. Rev.* B **99** 224509
[23] Kovacic M, Christensen M H, Gastiasoro M N and Andersen B M 2015 *Phys. Rev.* B **91** 064424
[24] Singh A 1991 *Phys. Rev.* B **43** 3617
[25] Carlson J 1989 *Phys. Rev.* B **40** 846
[26] Reger J D and Young A P 1988 *Phys. Rev.* B **37** 5978
[27] Hozoi L, Siurakshina L, Fulde P and van den Brink J 2011 *Sci. Rep.* **1** 65
[28] de Graaf C and Broer R 2000 *Phys. Rev.* B **62** 702
[29] Sala M M *et al* 2011 *New J. Phys.* **13** 043026
[30] Braicovich L *et al* 2009 *Phys. Rev. Lett.* **102** 167401
[31] Lorenzana J and Sawatzky G A 1995 *Phys. Rev. Lett.* **74** 1867
[32] Hill J P *et al* 2008 *Phys. Rev. Lett.* **100** 097001
[33] Perkins J D, Graybeal J M, Kastner M A, Birgeneau R J, Falck J P and Greven M 1993 *Phys. Rev. Lett.* **71** 1621
[34] Cox D L, Jarrell M, Jayaprakash C, Krishnamurthy H R and Deisz J 1989 *Phys. Rev. Lett.* **62** 2188
[35] Ohta Y, Tohyama T and Maekawa S 1991 *Phys. Rev.* B **43** 2968
[36] Eskes H and Sawatzky G A 1991 *Phys. Rev.* B **44** 9656
[37] Pavarini E, Dasgupta I, Saha-Dasgupta T, Jepsen O and Andersen O K 2001 *Phys. Rev. Lett.* **87** 047003
[38] de' Medici L 2011 *Phys. Rev.* B **83** 205112
[39] Georges A, de' Medici L and Mravlje J 2013 *Annu. Rev. Condens. Matter Phys.* **4** 137
[40] Fanfarillo L and Bascones E 2015 *Phys. Rev.* B **92** 075136
[41] de' Medici L, Giovannetti G and Capone M 2014 *Phys. Rev. Lett.* **112** 177001
[42] Yu R and Si Q 2012 *Phys. Rev.* B **86** 085104
[43] Knolle J, Eremin I and Moessner R 2011 *Phys. Rev.* B **83** 224503
[44] Coldea R, Hayden S M, Aeppli G, Perring T G, Frost C D, Mason T E, Cheong S-W and Fisk Z 2001 *Phys. Rev. Lett.* **86** 5377
[45] Kamble B and Singh A 2009 *Phys. Rev.* B **79** 064410
[46] Singh D K, Kamble B and Singh A 2010 *Phys. Rev.* B **81** 064430
[47] Raghuvanshi N and Singh A 2011 *J. Phys.: Condens. Matter* **23** 312201
[48] Singh D K 2017 *J. Appl. Phys.* **122** 073906
[49] Singh D K 2017 *J. Phys.: Condens. Matter* **29** 415601
[50] Headings N S, Hayden S M, Coldea R and Perring T G 2010 *Phys. Rev. Lett.* **105** 247001
[51] Horio M *et al* 2018 *Phys. Rev. Lett.* **121** 077004
[52] Weber C, Haule K and Kotliar G 2010 *Phys. Rev.* B **82** 125107